

Nucleon pole contribution in the $pp \rightarrow ppK^+K^-$ reaction below the ϕ meson threshold

Qi-Fang Lü,¹ Ju-Jun Xie,^{2,3,4,*} and De-Min Li^{1,†}

¹Department of Physics, Zhengzhou University, Zhengzhou, Henan 450001, China

²Institute of Modern Physics, Chinese Academy of Sciences, Lanzhou 730000, China

³Research Center for Hadron and CSR Physics, Institute of Modern Physics of CAS and Lanzhou University, Lanzhou 730000, China

⁴State Key Laboratory of Theoretical Physics, Institute of Theoretical Physics, Chinese Academy of Sciences, Beijing 100190, China

(Received 27 April 2014; published 8 September 2014)

Nucleon pole contribution in the $pp \rightarrow ppK^+K^-$ reaction below the threshold of the production of the ϕ meson is studied within the effective Lagrangian approach. It is assumed that the K^-p final state originates from the decay of the hyperons $\Lambda(1115)$ and $\Lambda(1405)$. In addition to the pp final state interaction (FSI) parametrized using the Jost function, we have also considered the K^+K^- FSI with the techniques of the chiral unitary approach, where the scalar mesons $f_0(980)$ and $a_0(980)$ were dynamically generated. Hence, the contributions from scalar mesons $f_0(980)$ and $a_0(980)$ occur through the K^+K^- FSI. It is shown that the available experimental data are well reproduced, especially the total cross sections and the invariant mass distributions of pp and K^+K^- . Furthermore, different forms of the couplings (pseudoscalar and pseudovector) for the πNN interaction and different strengths for the proton-proton FSI are also investigated. It is found that the contributions from hyperons $\Lambda(1115)$ and $\Lambda(1405)$ are different between these two kinds of couplings. On the other hand, the effects of the proton-proton FSI can be adjusted by the cutoff parameters used in the form factors.

DOI: [10.1103/PhysRevC.90.034002](https://doi.org/10.1103/PhysRevC.90.034002)

PACS number(s): 13.75.-n, 14.20.Gk, 13.30.Eg, 25.40.Ve

I. INTRODUCTION

The meson production reaction in nucleon-nucleon collisions near threshold has the potential to yield information on hadron properties [1], and also plays an important role for exploring the baryon spectroscopy [2]. In recent years, the experimental database on the reaction of $pp \rightarrow ppK^+K^-$ near threshold has been expanded significantly. In addition to the measurements of the $pp \rightarrow ppK^+K^-$ total and differential cross sections, below the threshold of the production of the ϕ meson, performed experimentally with COSY-11 [3,4] and ANKE [5] detectors at the cooler synchrotron COSY in Germany, there are invariant mass distributions of various subsystems obtained at excess energies $\varepsilon = 10, 23.9,$ and 28 MeV [5,6] and in Dalitz plots [6,7]. The total and differential cross sections are also available for the $pp \rightarrow ppK^+K^-$ reaction above the ϕ meson threshold determined by the ANKE [8,9] Collaboration and the DISTO [10] Collaboration.

In response to this wealth of data there have been theoretical investigations for the $pp \rightarrow ppK^+K^-$ reaction above ϕ meson production [11–13]. However, the theoretical investigations of this reaction below the ϕ meson threshold are scarce. Below the ϕ meson threshold, the main contribution to the production of K^+K^- pairs could be through the scalar mesons $a_0(980)$ and $f_0(980)$; thus, the original motivation for the study of the $pp \rightarrow ppK^+K^-$ reaction near threshold was to investigate the enigmatic properties of the scalar resonances $a_0(980)$ and $f_0(980)$ [5,6].

Unlike the production of the ϕ meson above threshold, in the low energy region we do not need to separate the non- ϕ from the ϕ contribution, and the fact that the data were spread

over a wide range of K^+K^- invariant masses gives a special advantage to investigation of the scalar mesons $a_0(980)$ and $f_0(980)$ [5]. These two mesons, which have been studied by a large number of theoretical works, are commonly explained as conventional $q\bar{q}$ mesons in the constituent quark model [14], tetraquark states by Jaffe [15], and $K\bar{K}$ molecules [16]. Besides, within the chiral unitary approach, the $f_0(980)$ and $a_0(980)$ scalar mesons are dynamically generated from the interaction of $K\bar{K}, \pi\pi,$ and $\eta\pi$ treated as coupled channels in $I = 0$ and $I = 1$, respectively [17–22]. Both couple strongly to the $K\bar{K}$ channel. Inspired by those results obtained from the chiral unitary approach, for the $pp \rightarrow ppK^+K^-$ reaction we take the final state interaction (FSI) between K^+ and K^- into account by using the techniques of the chiral unitary approach as in Refs. [17,23]. In this sense the contributions from scalar mesons $f_0(980)$ and $a_0(980)$ occur through the K^+K^- FSI. This approach has been used in the investigation of the FSI of mesons in different processes in order to get a better understanding of the nature of the meson resonances as shown in Refs. [24–27].

It has been suggested that the $\Lambda(1405)$ could play an essential role on the kaon pair production through the $pp \rightarrow pK^+(\Lambda(1405) \rightarrow K^-p)$ process [28], and this process seems more important than the contributions from the scalar mesons [11,29]. Indeed, the role played by the $\Lambda(1405)$ state is crucial for reproducing the K^-p mass distribution [12,30]. In Ref. [12], the reaction $pp \rightarrow ppK^+K^-$ has been studied by assuming that the K^-p final state originates from the decay of the $\Lambda(1405)$, where the $N_{1/2}^*(1535)$ resonance acts as a doorway state for the production of $\Lambda(1405)$. However, the model calculations of Ref. [12] underestimate the total cross sections of the $pp \rightarrow ppK^+K^-$ reaction near the kinematical threshold (see Fig. 4 of Ref. [12]). So, in the present work, within the effective Lagrangian approach, we restudy the $pp \rightarrow ppK^+K^-$ reaction below the threshold of the ϕ meson

*xiejujun@impcas.ac.cn

†lidm@zzu.edu.cn

production by considering the contribution from the nucleon pole. Additionally, different forms of the couplings (pseudoscalar and pseudovector) for the πNN interaction and different strengths for the proton-proton FSI are also investigated.

In the next section, we will present the formalism and ingredients necessary for our estimations, then numerical results and discussions are given in Sec. III. Finally, a short summary is given in the last section.

II. FORMALISM AND INGREDIENTS

We study the $pp \rightarrow ppK^+K^-$ reaction below the threshold of the production of the ϕ meson within an effective Lagrangian approach. The basic Feynman diagrams for this process are depicted in Fig. 1, where we pay attention to the contribution from the nucleon pole for the production of the $K\Lambda(1115)$ pair and $K\Lambda(1405)$ pair, while the K^-p pair is produced by the decay of the off-shell $\Lambda(1115)$ and the subthreshold $\Lambda(1405)$ ($\equiv \Lambda^*$). Because of the large πNN coupling and the small pion mass, the underlying mechanism will be dominated by the π^0 exchange. Thus, the contributions from the η , ρ , and ω exchanges are neglected in the present calculation.

To compute the amplitudes of these diagrams shown in Fig. 1, we need the effective Lagrangian densities for the interaction vertexes. There are two forms for πNN interaction commonly employed in the literature [31]. One is the pseudoscalar (PS) coupling,

$$\mathcal{L}_{\pi NN}^{\text{PS}} = -ig_{\pi NN} \bar{\psi}_N \gamma_5 \vec{\tau} \cdot \vec{\pi} \psi_N, \quad (1)$$

and the other one is the pseudovector (PV) coupling,

$$\mathcal{L}_{\pi NN}^{\text{PV}} = -\frac{g_{\pi NN}}{2m_N} \bar{\psi}_N \gamma_5 \gamma_\mu \vec{\tau} \cdot \partial^\mu \vec{\pi} \psi_N. \quad (2)$$

Following the SU(3) flavor symmetry, the $KN\Lambda$ interaction Lagrangian densities are similar to the πNN interaction,

$$\mathcal{L}_{KN\Lambda}^{\text{PS}} = -ig_{KN\Lambda} \bar{\psi}_N \gamma_5 K \psi_\Lambda + \text{H.c.}, \quad (3)$$

$$\mathcal{L}_{KN\Lambda}^{\text{PV}} = -\frac{g_{KN\Lambda}}{m_N + m_\Lambda} \bar{\psi}_N \gamma_5 \gamma_\mu \partial^\mu K \psi_\Lambda + \text{H.c.} \quad (4)$$

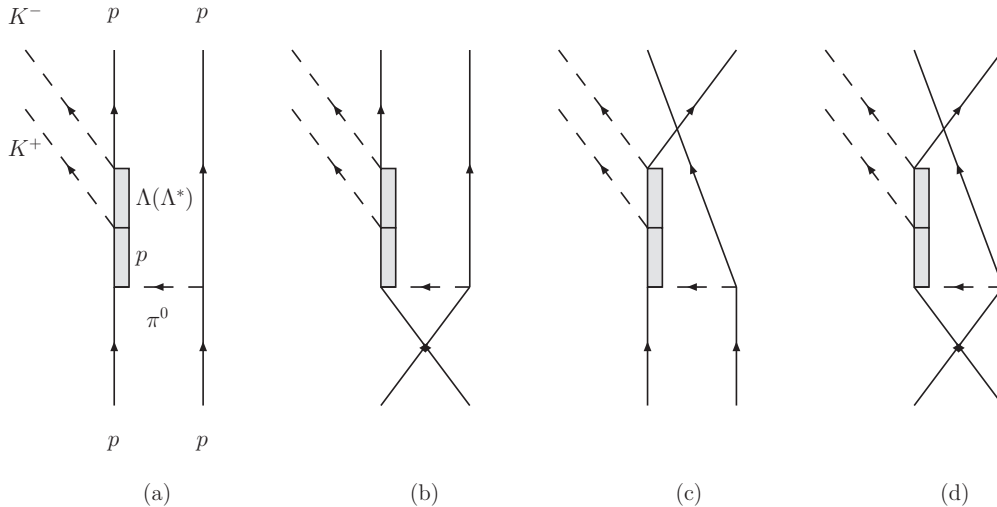


FIG. 1. Feynman diagrams for the $pp \rightarrow ppK^+K^-$ reaction.

In addition, the effective $KN\Lambda(1405)$ coupling is also needed [32]:

$$\mathcal{L}_{KN\Lambda^*} = -ig_{KN\Lambda^*} \bar{\psi}_N K \psi_{\Lambda^*} + \text{H.c.} \quad (5)$$

The coupling constants in the above Lagrangian densities are taken as [32] $g_{\pi NN} = 13.45$, $g_{KN\Lambda} = -13.98$, and $g_{KN\Lambda^*} = 1.51$.

On the other hand, we need to include the form factors because the hadrons are not point-like particles. We adopt here the common scheme used in many previous works. In our calculation, for the πNN vertex, we take the form following that used in Refs. [33–35],

$$F_\pi(k_\pi^2) = \frac{\Lambda_\pi^2 - m_\pi^2}{\Lambda_\pi^2 - k_\pi^2}, \quad (6)$$

where k_π , m_π , and Λ_π are the four-momentum, mass, and cutoff parameter for the exchanged pion meson, respectively. For the cutoff parameter Λ_π , we take the value of 1.3 GeV [36,37].

The form factors for the off-shell nucleon and the hyperon $\Lambda(1115)$ and $\Lambda(1405)$ states are taken in the form advocated in Refs. [38–40],

$$F(q_{ex}^2, M_{ex}) = \frac{\Lambda^4}{\Lambda^4 + (q_{ex}^2 - M_{ex}^2)^2}, \quad (7)$$

where q_{ex} and M_{ex} are the four-momentum and the mass of the exchanged hadron, respectively. In the present calculation, to minimize the number of free parameters, we use the same cutoff parameters for those hadrons for simplicity, i.e., $\Lambda_N = \Lambda_\Lambda = \Lambda_{\Lambda^*} = \Lambda$. The value of the cutoff parameter will be discussed in the following.

Then, according to the Feynman rules, the scattering amplitudes for the $pp \rightarrow ppK^+K^-$ reaction can be obtained straightforwardly with the above effective couplings. Here, we give explicitly the amplitude of Fig. 1(a) with $\Lambda(1115)$ exchange and in the case of PS coupling for πNN and

$KN\Lambda(1115)$ vertexes as an example:

$$\begin{aligned} \mathcal{M}_a^\Lambda &= g_{\pi NN}^2 g_{KN\Lambda}^2 F_\pi^2(k_\pi^2) F(q_1^2, m_N) F(q_2^2, m_\Lambda) G_\pi(k_\pi) \\ &\quad \times \bar{u}(p_4, s_4) \gamma_5 G_\Lambda(q_\Lambda) \gamma_5 G_N(q_N) \gamma_5 u(p_1, s_1) \\ &\quad \times \bar{u}(p_3, s_3) \gamma_5 u(p_2, s_2), \end{aligned} \quad (8)$$

where s_i ($i = 1, 2, 3, 4$) and p_i ($i = 1, 2, 3, 4$) represent respectively the spin projection and four-momentum of the initial or final protons; $G_\pi(k_\pi)$ [$G_N(q_N)$] is the propagator for the exchanged π meson [nucleon].

The π meson propagator used in our calculation is

$$G_\pi(k_\pi) = \frac{i}{k_\pi^2 - m_\pi^2}, \quad (9)$$

The propagators of the nucleon and $\Lambda(1115)$ can be written as

$$G_{N/\Lambda}(q_{N/\Lambda}) = \frac{i(\not{q}_{N/\Lambda} + m_{N/\Lambda})}{q_{N/\Lambda}^2 - m_{N/\Lambda}^2}, \quad (10)$$

where the q_N [q_Λ] is the four-momentum of the intermediate nucleon [$\Lambda(1115)$].

In addition, the propagator of the $\Lambda(1405)$ resonance is written in a Breit-Wigner form [41],

$$G_{\Lambda^*}(q) = \frac{i(\not{q} + m_{\Lambda^*})}{q^2 - m_{\Lambda^*}^2 + im_{\Lambda^*}\Gamma_{\Lambda^*}(q^2)}, \quad (11)$$

where $\Gamma_{\Lambda^*}(q^2)$ is the energy-dependent total width of the Λ^* resonance, which can be expressed as [32]

$$\begin{aligned} \Gamma_{\Lambda^*}(q^2) &= \frac{3g_{\Lambda^*\pi\Sigma}^2}{4\pi}(E_\Sigma + m_\Sigma) \frac{|\vec{p}_\Sigma|}{\sqrt{q^2}} + \frac{g_{\Lambda^*\bar{K}N}^2}{2\pi}(E_N + m_N) \\ &\quad \times \frac{|\vec{p}_N|}{\sqrt{q^2}} \theta(\sqrt{q^2} - m_{\bar{K}} - m_N), \end{aligned} \quad (12)$$

with

$$E_{\Sigma/N} = \frac{q^2 + m_{\Sigma/N}^2 - m_{\pi/\bar{K}}^2}{2\sqrt{q^2}}, \quad (13)$$

$$|\vec{p}_{\Sigma/N}| = \sqrt{E_{\Sigma/N}^2 - m_{\Sigma/N}^2}. \quad (14)$$

According to Fig. 1, the full invariant amplitude for the $pp \rightarrow ppK^+K^-$ reaction through the proton and $\Lambda(1115)$ [proton and $\Lambda(1405)$] is composed of four parts:

$$\mathcal{M}_0 = \sum_{i=a,b,c,d} \eta_i \mathcal{M}_i, \quad (15)$$

with the factors $\eta_a = \eta_d = 1$ and $\eta_b = \eta_c = -1$.

The final state interaction for the final K^+K^- subsystem is given by the meson-meson amplitude from the lowest order chiral Lagrangian with the chiral unitary approach as in Ref. [17]. We choose five channels K^+K^- , $K^0\bar{K}^0$, $\pi^+\pi^-$, $\pi^0\pi^0$ and $\pi^0\eta$, which are denoted from 1 to 5, to calculate the amplitude $T_{K^+K^- \rightarrow K^+K^-}$ in the charge eigenstates directly.

The scattering amplitude $T_{K^+K^- \rightarrow K^+K^-}$ can be obtained by solving the Bathe-Salpeter equation,¹

$$T = [1 - VG]^{-1}V, \quad (16)$$

where G is a diagonal matrix with the matrix elements

$$\begin{aligned} G_{ii} &= i \int \frac{d^4q}{(2\pi)^4} \frac{1}{q^2 - m_{i_1}^2 + i\epsilon} \frac{1}{(P-q)^2 - m_{i_2}^2 + i\epsilon} \\ &= \int_0^{q_{\max}} \frac{q^2 dq}{(2\pi)^2} \frac{\omega_1 + \omega_2}{\omega_1 \omega_2 [P^{02} - (\omega_1 + \omega_2)^2 + i\epsilon]}, \end{aligned} \quad (17)$$

where P is the total four-momentum of the meson-meson system and q is the four-momentum of one of the intermediate mesons with $\omega_i = (\vec{q}^2 + m_i^2)^{1/2}$. The loop integration variable is regularized with a cutoff $|\vec{q}| < q_{\max}$ and $q_{\max} = 1030$ MeV as used in Refs. [17,23]. With this value, the scalar mesons $f_0(980)$ and $a_0(980)$ were dynamically generated as poles of the S -wave amplitudes. Thus, in the present case, the contributions from scalar mesons $f_0(980)$ and $a_0(980)$ occur via the FSI between K^+ and K^- .

For the FSI of the proton and proton in the final state, we use the general framework based on the Jost function formalism,

$$J(k)^{-1} = \frac{k + i\beta}{k - i\alpha}, \quad (18)$$

where k is the internal momentum of the pp subsystem. In this case, we use two sets of parameters. One is the widely used 1S_0 pp interaction, with $\alpha = -20.5$ MeV and $\beta = 166.7$ MeV [42,43]. The other is $\alpha = 0.1$ fm⁻¹ and $\beta = 0.5$ fm⁻¹ (corresponding to $\alpha = 19.7$ MeV and $\beta = 98.7$ MeV) as used in Ref. [8].

Taking the FSI of K^+K^- and pp subsystems into account, the amplitude of the $pp \rightarrow ppK^+K^-$ reaction can be written as²

$$\mathcal{M} = (\mathcal{M}_0 + \mathcal{M}_0 G_{K^+K^-} T_{K^+K^- \rightarrow K^+K^-}) J(k)^{-1}. \quad (19)$$

Then the calculations of the invariant scattering amplitude $|\mathcal{M}|^2$ and the cross sections for $pp \rightarrow ppK^+K^-$ reaction are straightforward:

$$\begin{aligned} d\sigma(pp \rightarrow ppK^+K^-) &= \frac{1}{4} \frac{m_p^2}{F} \sum_{s_1, s_2} \sum_{s_3, s_4} |\mathcal{M}|^2 \frac{m_p d^3 p_3}{E_3} \frac{m_p d^3 p_4}{E_4} \frac{d^3 p_{K^+}}{2E_{K^+}} \frac{d^3 p_{K^-}}{2E_{K^-}} \\ &\quad \times \frac{1}{2} \delta^4(p_1 + p_2 - p_3 - p_4 - p_{K^+} - p_{K^-}), \end{aligned} \quad (20)$$

where E_3 and E_4 are the energies of the final protons; p_{K^+} and E_{K^+} (p_{K^-} and E_{K^-}) stand for the four-momentum and energy of the final state K^+ (K^-), respectively. The factor $\frac{1}{2}$ before the δ function comes from the two identical protons in the final

¹As shown in Ref. [17], the scattering amplitude $T_{K^+K^- \rightarrow K^+K^-}$ is projected to be S wave.

²It is worth mentioning that the loop function $G_{K^+K^-}$ and the amplitude $T_{K^+K^- \rightarrow K^+K^-}$ only depend on the invariant mass of the K^+K^- subsystem.

state, while the flux factor F in the above equation is

$$F = (2\pi)^8 \sqrt{(p_1 p_2)^2 - m_p^4}. \quad (21)$$

Since the relative phase between $\Lambda(1115)$ and $\Lambda(1405)$ exchanges is not known, the interference terms between these parts could be small, and are ignored in our concrete calculation.

III. NUMERICAL RESULTS AND DISCUSSIONS

With the formalism and ingredients given above, the total cross section versus excess energy ε for the $pp \rightarrow ppK^+K^-$ reaction is calculated by using a Monte Carlo multiparticle phase space integration program. The results for ε from the reaction threshold to 30 MeV, which is just below the ϕ threshold ($\varepsilon = 32$ MeV), and the experimental data taken from Refs. [3–5], are shown in Fig. 2. In our calculation, we take two types (PS and PV) of πNN and $KN\Lambda$ couplings, and two sets of proton-proton FSI parameters. Therefore, there are a total of four combinations as shown in Table I.

In Fig. 2, the solid, dashed, dotted, and dot-dashed curves stand for our theoretical results obtained with the parameters of Sets I, II, III, and IV, respectively. Because of the large error bars of the experimental data points, from Fig. 2 one can see that, with the cutoff parameters of form factors for exchanged hadrons in the different sets listed in Table I, we can reproduce the experimental data on the total cross sections of the $pp \rightarrow ppK^+K^-$ reaction. Also, one can see that, although the absolute values of those parameters of different sets have some discrepancies, they all can fairly well describe the experimental data, but the trends of the results obtained with PS and PV coupling are different.

However, the contributions of $\Lambda(1115)$ and $\Lambda(1405)$ are different between PS and PV couplings. These results are

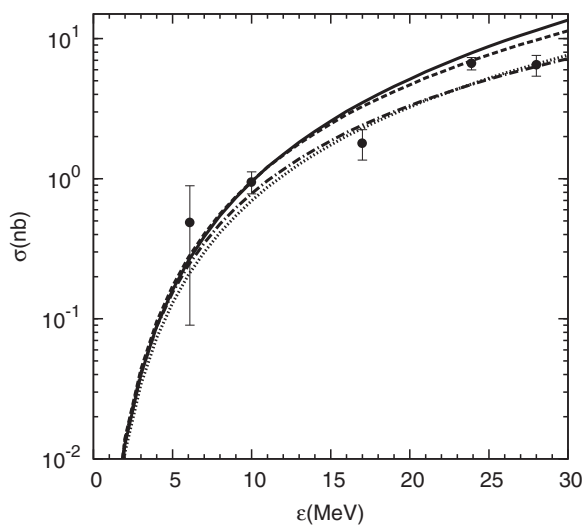


FIG. 2. Total cross sections vs excess energies (ε) for the $pp \rightarrow ppK^+K^-$ reaction from the present calculation. The experimental data are taken from Refs. [3–5]. The solid, dashed, dotted, and dot-dashed curves stand for the results obtained with the parameters of Sets I, II, III, and IV, respectively.

TABLE I. Parameters used in the present calculation.

Set	πNN and $KN\Lambda$ couplings	pp FSI (MeV)	Cutoff (GeV)
I	PS	$\alpha = 19.7, \beta = 98.7$	1.5
II	PS	$\alpha = -20.5, \beta = 166.7$	1.3
III	PV	$\alpha = 19.7, \beta = 98.7$	1.5
IV	PV	$\alpha = -20.5, \beta = 166.7$	1.3

depicted in Fig. 3, where the dashed and dotted lines stand for contributions from $\Lambda(1115)$ and $\Lambda(1405)$, respectively. The results shown in individual panels (a), (b), (c), and (d) are obtained with Sets I, II, III, and IV. It is shown that the $\Lambda(1115)$ hyperon plays a dominant role in the case of PS coupling, while the $\Lambda(1405)$ also has a significant contribution. In contrast, in the case of PV coupling, the $\Lambda(1405)$ contribution is predominant while the $\Lambda(1115)$ hyperon contribution is rather small and can be neglected.

Since we only pay attention to the $pp \rightarrow ppK^+K^-$ reaction below the threshold of the production of the ϕ meson and also near the $\Lambda(1405)$ threshold, it is expected that $\Lambda(1405)$ would play an important role in this energy region [8,12,30]. Although the PS coupling can also reproduce the total cross section data, it seems that the PV coupling is more favored. As shown in Ref. [31], the PV coupling is more general than the PS coupling. Besides, it is also shown that, for the $pp \rightarrow ppK^+K^-$ reaction, the effect of the pp FSI on the total cross section can be adjusted by modifying the cutoff parameters in the form factors of the intermediate proton and $\Lambda(1115)$.

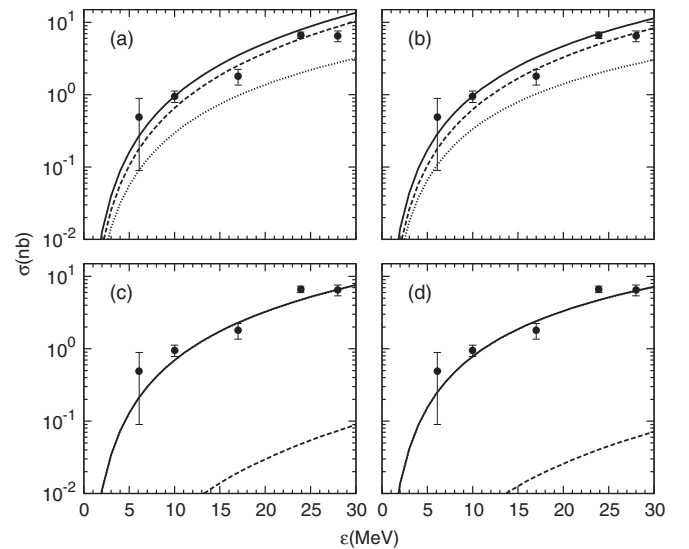


FIG. 3. Total cross sections for the $pp \rightarrow ppK^+K^-$ reaction. The experimental data are taken from Refs. [3–5]. The dashed and dotted lines stand for contributions from $\Lambda(1115)$ and $\Lambda(1405)$, respectively. The individual panels are (a) results obtained with Set I, (b) results obtained with Set II, (c) results obtained with Set III, and (d) results obtained with Set IV.

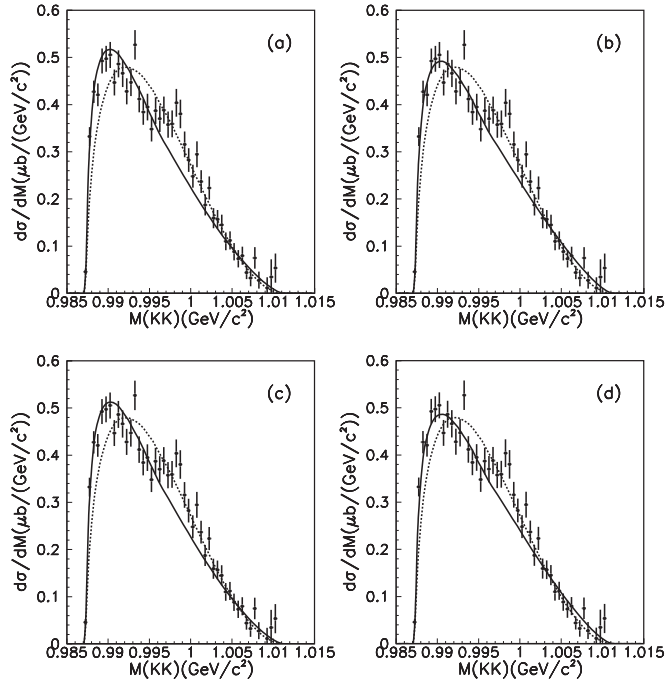


FIG. 4. The K^+K^- invariant mass distribution (solid lines) at the excess energy of $\varepsilon = 23.9$ MeV compared with the experimental data [5] and phase space distribution (dashed lines). The panels (a), (b), (c), and (d) denote the results obtained from Set I, II, III, and IV, respectively.

To show the effect from the K^+K^- FSI, we give the results for the K^+K^- invariant mass spectrum of the $pp \rightarrow ppK^+K^-$ reaction at an excess energy $\varepsilon = 23.9$ MeV in Fig. 4, where panels (a), (b), (c), and (d) stand for the results obtained with the parameters of Sets I, II, III and, IV, respectively. In Fig. 4, the dashed lines are pure phase space distributions, while the solid lines are full calculations from our model. By comparing our theoretical results with the experimental data, we found that the K^+K^- FSI employed within a chiral unitary approach plays an essential role in describing the line shape of the K^+K^- . The peak near the K^+K^- threshold can be well reproduced by including the K^+K^- FSI with the techniques of the chiral unitary approach, where the scalar mesons $f_0(980)$ and $a_0(980)$ were dynamically generated. In this sense, the $f_0(980)$ and $a_0(980)$ mesons play an important role in the $pp \rightarrow ppK^+K^-$ reaction below the threshold of the production of the ϕ meson. Furthermore, the pp FSI can also slightly influence the K^+K^- invariant mass distribution. Here, we find again that the PS and PV couplings are both good enough to reproduce the experimental data, and the effects of pp FSI on the differential cross sections can also be adjusted by the cutoff parameters.

Finally, in Figs. 5 and 6, with the parameters of Set III, we give our model predictions of the differential cross sections for the $pp \rightarrow ppK^+K^-$ reaction at excess energies $\varepsilon = 10$ and $\varepsilon = 28$ MeV together with experimental data [6]. It is shown that our theoretical calculations can reasonably describe the experimental data at both excess energies $\varepsilon = 10$ and $\varepsilon = 28$ MeV, especially for the K^+K^- and pp invariant mass

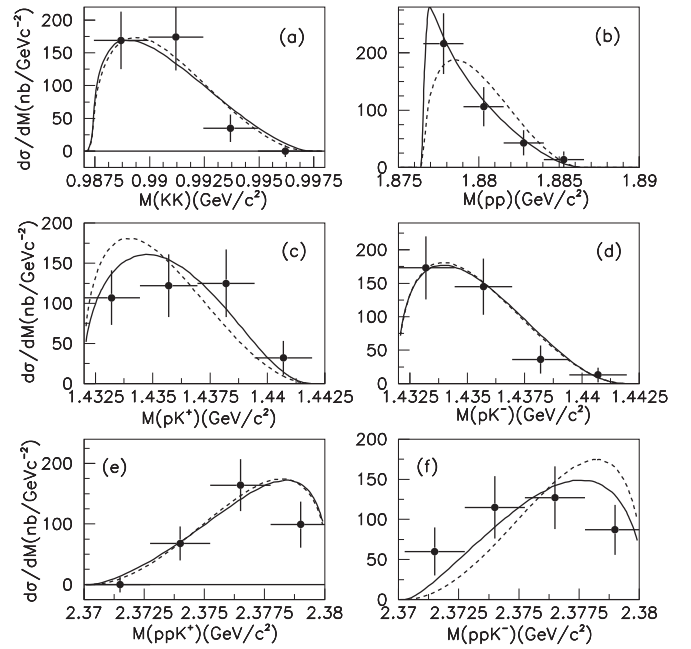


FIG. 5. Differential cross section for the $pp \rightarrow ppK^+K^-$ reaction at the excess energy of $\varepsilon = 10$ MeV compared with the experimental data [6]. The solid curves stand for our theoretical calculations while the dashed lines represent the pure phase space distribution.

distributions, which is because we have included both the K^+K^- FSI and the pp FSI.

From Fig. 6, one can see that, although we have considered the contributions from the $\Lambda(1405)$ state, we still cannot well reproduce the invariant K^-p mass distribution. This

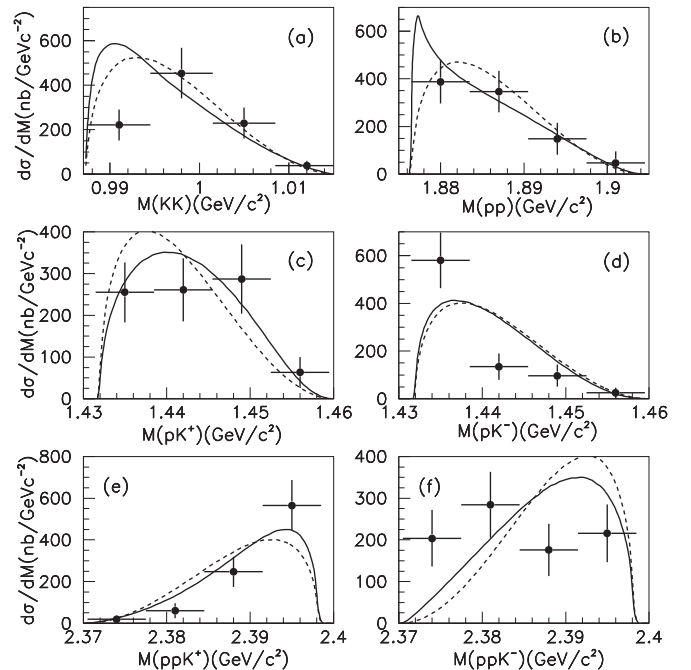


FIG. 6. As in Fig. 5 but at the excess energy of $\varepsilon = 28$ MeV.

indicates the strong K^-p FSI. In Ref. [30], the role of the two $\Lambda(1405)$ states which are dynamically generated from the $\bar{K}N$ and $\pi\Sigma$ chiral interactions [44–46] is investigated at a proton beam $p_{\text{lab}} = 3.65$ GeV (corresponding to $\varepsilon = 108$ MeV for the case of the $pp \rightarrow ppK^+K^-$ reaction). It is shown that the kaon-exchange term, which is mostly dominated by the high energy $\Lambda(1405)$ pole, is crucial to produce the line shape of the $\pi^0\Sigma^0$ [$\Lambda(1405) \rightarrow \pi^0\Sigma^0$]. Thus, the kaon-exchange mechanism should be also important in the present case, especially for producing the line shape of the K^-p . However, our model can give a reasonable description of the experimental data on the total cross section and most differential cross sections in the considered energy region. Meanwhile, our calculation offers some important clues for the mechanisms of the $pp \rightarrow ppK^+K^-$ reaction and makes a first effort to study the K^+K^- FSI with the chiral unitary approach. Hence, we will leave the issue of the strong K^-p FSI to further studies.

IV. SUMMARY AND CONCLUSIONS

In this work, we have investigated the $pp \rightarrow ppK^+K^-$ reaction within an effective Lagrangian model. With the assumption that the kaon pair production is mainly through the nucleon pole, $\Lambda(1115)$, and $\Lambda(1405)$, our calculation can reproduce the total cross section at the energy region below the threshold of the production of the ϕ meson.

We adopted the pseudoscalar and pseudovector couplings for the πNN interaction. It is found that both pseudoscalar and pseudovector couplings can describe the experimental data, but the $\Lambda(1115)$ plays an important role in the case of the PS coupling, while the $\Lambda(1405)$ contribution is predominant for

the PV coupling. However, considering the contributions from the $\Lambda(1405)$ state, we still cannot well reproduce the invariant K^-p mass distribution, which indicates the strong K^-p FSI.

In addition to the pp FSI using the Jost function, the K^+K^- FSI is also studied with the chiral unitary approach, where the scalar mesons $f_0(980)$ and $a_0(980)$ were dynamically generated as poles of the S -wave amplitudes. In this sense the roles of mesons $f_0(980)$ and $a_0(980)$ are played through the K^+K^- FSI. After taking the pp and K^+K^- FSI into account, the experimental data on the invariant mass distributions of the pp and K^+K^- are well reproduced at an excess energy $\varepsilon = 23.9$ MeV. Besides, it can also be seen that the contribution from the isospin-zero channel is much stronger than the isospin-one channel in the $K^+K^- \rightarrow K^+K^-$ process in a chiral unitary approach [17], which agrees with the experiment data analysis given by Ref. [5].

It is evident that the FSI of the four-body ppK^+K^- is extremely complex. Nevertheless, taking the pp and K^+K^- FSI into account, the energy dependence of the total cross sections below the threshold of the production of the ϕ meson can be well reproduced by considering the contributions from the nucleon pole, $\Lambda(1115)$, and $\Lambda(1405)$. However, the strong K^-p FSI still requires study by further theoretical works because it always connected with the controversial $\Lambda(1405)$ state.

ACKNOWLEDGMENTS

We warmly thank Qiujian Ye for sending us the experimental data files, and Xu Cao for helpful discussions. This work is partly supported by the National Natural Science Foundation of China under Grant No. 11105126, and the Scientific Research Foundation for the Returned Overseas Chinese Scholars, State Education Ministry.

-
- [1] C. Hanhart, *Phys. Rep.* **397**, 155 (2004).
 - [2] B. S. Zou, *Chin. Phys. C* **33**, 1113 (2009), and references therein.
 - [3] C. Quentmeier, H. H. Adam, J. T. Balewski, A. Budzanowski, D. Grzonka, L. Jarczyk, A. Khoukaz, K. Kilian *et al.*, *Phys. Lett. B* **515**, 276 (2001).
 - [4] P. Winter, M. Wolke, H.-H. Adam, A. Budzanowski, R. Czyzykiewicz, D. Grzonka, M. Janusz, L. Jarczyk *et al.*, *Phys. Lett. B* **635**, 23 (2006).
 - [5] Q. J. Ye, M. Hartmann, D. Chiladze, S. Dymov, A. Dzyuba, H. Gao, R. Gebel, V. Hejny *et al.*, *Phys. Rev. C* **87**, 065203 (2013).
 - [6] M. Silarski *et al.* (COSY-11 Collaboration), *Phys. Rev. C* **80**, 045202 (2009).
 - [7] M. Silarski and P. Moskal, *Phys. Rev. C* **88**, 025205 (2013).
 - [8] Y. Maeda *et al.* (ANKE Collaboration), *Phys. Rev. C* **77**, 015204 (2008).
 - [9] Q. J. Ye, M. Hartmann, Y. Maeda, S. Barsov, M. Buscher, D. Chiladze, S. Dymov, A. Dzyuba *et al.*, *Phys. Rev. C* **85**, 035211 (2012).
 - [10] F. Balestra *et al.* (DISTO Collaboration), *Phys. Lett. B* **468**, 7 (1999).
 - [11] A. Dzyuba, M. Buscher, M. Hartmann, I. Keshelashvili, V. Koptev, Y. Maeda, A. Sibirtsev, H. Stroher *et al.*, *Phys. Lett. B* **668**, 315 (2008).
 - [12] J.-J. Xie and C. Wilkin, *Phys. Rev. C* **82**, 025210 (2010).
 - [13] P. Lebiedowicz and A. Szczurek, *Phys. Rev. D* **85**, 014026 (2012).
 - [14] D. Morgan and M. R. Pennington, *Phys. Rev. D* **48**, 1185 (1993).
 - [15] R. L. Jaffe, *Phys. Rev. D* **15**, 267 (1977).
 - [16] J. D. Weinstein and N. Isgur, *Phys. Rev. D* **41**, 2236 (1990).
 - [17] J. A. Oller and E. Oset, *Nucl. Phys. A* **620**, 438 (1997); **652**, 407 (1999).
 - [18] J. A. Oller, E. Oset, and J. R. Pelaez, *Phys. Rev. Lett.* **80**, 3452 (1998).
 - [19] J. A. Oller and E. Oset, *Phys. Rev. D* **60**, 074023 (1999).
 - [20] A. Gomez Nicola and J. R. Pelaez, *Phys. Rev. D* **65**, 054009 (2002).
 - [21] J. R. Pelaez and G. Rios, *Phys. Rev. Lett.* **97**, 242002 (2006).
 - [22] N. Kaiser, *Eur. Phys. J. A* **3**, 307 (1998).
 - [23] C.-B. Li, E. Oset, and M. J. Vicente Vacas, *Phys. Rev. C* **69**, 015201 (2004).
 - [24] E. Marco, S. Hirenzaki, E. Oset, and H. Toki, *Phys. Lett. B* **470**, 20 (1999).
 - [25] V. E. Markushin, *Eur. Phys. J. A* **8**, 389 (2000).
 - [26] J. E. Palomar, L. Roca, E. Oset, and M. J. Vicente Vacas, *Nucl. Phys. A* **729**, 743 (2003).

- [27] F.-K. Guo, P.-N. Shen, H.-C. Chiang, and R.-G. Ping, *Phys. Lett. B* **658**, 27 (2007).
- [28] C. Wilkin, *Acta Phys. Polon. Supp.* **2**, 89 (2009).
- [29] E. L. Bratkovskaya, W. Cassing, L. A. Kondratyuk, and A. Sibirtsev, *Eur. Phys. J. A* **4**, 165 (1999).
- [30] L. S. Geng and E. Oset, *Eur. Phys. J. A* **34**, 405 (2007).
- [31] W.-H. Liang, P.-N. Shen, B.-S. Zou, and A. Faessler, *Eur. Phys. J. A* **21**, 487 (2004).
- [32] J.-J. Xie, B.-C. Liu, and C.-S. An, *Phys. Rev. C* **88**, 015203 (2013).
- [33] R. Machleidt, K. Holinde, and C. Elster, *Phys. Rep.* **149**, 1 (1987).
- [34] R. Machleidt, *Adv. Nucl. Phys.* **19**, 189 (1989).
- [35] R. Brockmann and R. Machleidt, *Phys. Rev. C* **42**, 1965 (1990).
- [36] J.-J. Xie and B.-S. Zou, *Phys. Lett. B* **649**, 405 (2007).
- [37] J.-J. Xie, B.-S. Zou, and H.-C. Chiang, *Phys. Rev. C* **77**, 015206 (2008).
- [38] T. Feuster and U. Mosel, *Phys. Rev. C* **58**, 457 (1998); **59**, 460 (1999).
- [39] G. Penner and U. Mosel, *Phys. Rev. C* **66**, 055211 (2002); **66**, 055212 (2002).
- [40] V. Shklyar, H. Lenske, and U. Mosel, *Phys. Rev. C* **72**, 015210 (2005).
- [41] W. H. Liang, P. N. Shen, J. X. Wang, and B. S. Zou, *J. Phys. G* **28**, 333 (2002).
- [42] A. Sibirtsev and W. Cassing, *Eur. Phys. J. A* **7**, 407 (2000).
- [43] A. Sibirtsev, J. Haidenbauer, and U.-G. Meissner, *Eur. Phys. J. A* **27**, 263 (2006).
- [44] D. Jido, J. A. Oller, E. Oset, A. Ramos, and U. G. Meissner, *Nucl. Phys. A* **725**, 181 (2003).
- [45] V. K. Magas, E. Oset, and A. Ramos, *Phys. Rev. Lett.* **95**, 052301 (2005).
- [46] E. Oset, A. Ramos, and C. Bennhold, *Phys. Lett. B* **527**, 99 (2002); **530**, 260 (2002).